

Polarization Conversion in the Reflectivity Properties of Photonic Crystal Waveguides

Alan D. Bristow, Vasily N. Astratov, Ryoko Shimada, Ian S. Culshaw, Maurice S. Skolnick,
David M. Whittaker, Abbes Tahraoui, and Thomas F. Krauss

Abstract—Very strong resonant polarization conversion is observed in the reflectivity properties of one-dimensional lattices of air trenches deeply etched in AlGaAs surface waveguides. The symmetry properties and the magnitudes of the observed effects are found to be in very good agreement with the results of scattering matrix calculations.

Index Terms—Photonic Crystals, Photonic Band Structure, Reflectivity, Polarization, Waveguide, Electromagnetic Coupling.

I. INTRODUCTION

PHOTONIC crystal waveguides constitute a class of photonic crystal structures which exhibit band structure effects for guided modes [1] and in addition several novel external coupling properties for leaky modes [2-8]. Surface external coupling occurs under phase matching conditions when both the energy and the in-plane wave vector of incident light match those of the folded band structure of the photonic crystal modes. Such external coupling to leaky modes above the light line is manifested in external reflectivity spectra by the appearance of sharp resonant features and polarization mixing [4,7-11] and anticrossing between bands; by contrast in two dimensional (2D) photonic crystals of infinite vertical extent, without vertical waveguide confinement, such bands are pure transverse electric (TE) or transverse magnetic (TM) eigenstates of the electromagnetic field [12].

The polarization mixing of bands, leading to TE modes of the 2D crystal appearing in TM polarized reflectivity spectra [4,7] or vice versa, arises from the effects of zone folding and the vertical confinement. Band states which would otherwise lie outside the light cone, are folded back into the first Brillouin zone by the effects of the lattice potential. Since the lattice potential contains off diagonal components which mix pure TE and TM states, bands become observable in 'oppositely' polarized reflectivity spectra [4,7,13]. Two of us have also predicted that polarization conversion of incident TE_{in} (TM_{in}) polarized light into outgoing TM_{out} (TE_{out}) may

occur when light is incident away from the main symmetry directions of the photonic lattice [7]. Such *polarization conversion* was recently observed for 2D triangular lattices of air cylinders [13], with relatively modest polarization of the outgoing light, $\beta=TM_{out}/TE_{out}$ of order of ~ 1 .

In the present paper we report very strong polarization conversion effects in the reflectivity of a one-dimensional lattice of air trenches etched into an AlGaAs surface waveguide structure, of the type employed in refs [5,6]. We observe very strong polarizations of the outgoing beam of order $\beta = 4$, for directions of incidence away from the main symmetry directions of the lattice, with high efficiencies (TM_{out}/TM_{in}) of order 30%. We also show theoretically that the strength of the polarization conversion is a strong function of the depth of the lattice, and is negligibly small for e.g. shallow etched Bragg gratings.

The paper is organized as follows. After description of the samples and the measurement techniques in Section II, we present the determination of the photonic band structure in Sec. III. The polarization conversion effects are presented in Sec. IV. Finally we summarise the main conclusions in Sec. V.

II. EXPERIMENTAL

A. Samples

The samples studied in this work are surface waveguides with a 1D lattice of air trenches deep etched through the waveguide, as shown in Fig 1, to give rise to photonic band structure effects for the guided modes. The planar waveguides were grown using molecular beam epitaxy (MBE) and had $Al_{0.08}Ga_{0.92}As$ core thickness of $d = 240nm$, and were clad by air on the top side and $Al_{0.9}Ga_{0.1}As$, of thickness $d_{cl} = 790nm$ on the lower side.

1D lattices of air stripes of width $w = 45nm$ were fabricated by electron beam lithography and deep reactive ion etching (RIE), see Fig.1 (c). The air trenches were deep etched through the core into the cladding to depths $d_e \sim 450nm$ (aspect ratio ~ 10) to reduce scattering [5,6]. In this paper we focus on a lattice period of $a = 295nm$ and air fill factor $f = 22\%$ as determined by SEM (Fig.1 (b)), although lattices of several other periods and fill fractions were also investigated. The size of the lattices was $80\mu m \times 80\mu m$.

This work is funded by the EPSRC.

A. D. Bristow, V. N. Astratov, R. Shimada, I. S. Culshaw, D.M. Whittaker and M. S. Skolnick, are with the Department of Physics and Astronomy, University of Sheffield, Sheffield, S3 7RH, U.K. (e-mail: a.d.bristow@shef.ac.uk)

V. N. Astratov is also with the Department of Physics, University of North Carolina at Charlotte, Charlotte, North Carolina 28223, U.S.A.

R. Shimada is also with the Department of Physics, Japan Women's University, Tokyo 112-8681, Japan

A. Tahraoui and T. F. Krauss are with the School of Physics & Astronomy, University of St. Andrews, St. Andrews, Fife, KY16 9SS, U.K.

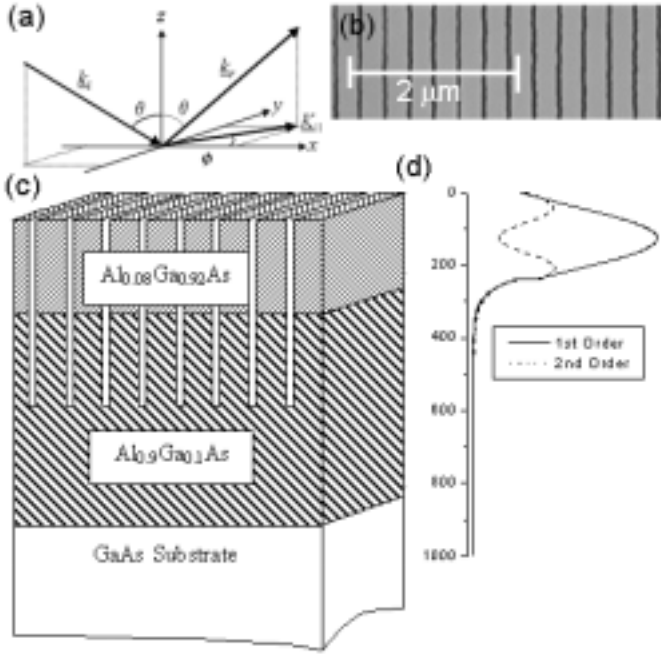


Fig 1. (a) Experimental geometry (b) Scanning electron micrograph of the surface of 1D lattice with period $a = 295\text{nm}$ and $f=22\%$. (c) Cross-sectional schematic (d) Depth dependent mode profile for 1st and 2nd order modes.

B. Experimental Geometry

Surface reflectivity spectra were obtained using linearly polarized TE incident light from a broadband tungsten-halogen lamp. To select the angle of incidence (θ , the polar angle, see Fig.1 (a)), the sample was illuminated with a highly collimated beam with angular spread $<1^\circ$. The angle of incidence was varied in a broad range from 0° to 70° .

The samples were positioned on a mount which could be rotated about a vertical axis, permitting additional control of the direction of incidence relative to the symmetry directions of the lattice, as defined by the azimuthal angle ϕ , see Fig.1(a). Incidence perpendicular to the air trenches corresponds to $\phi=0^\circ$ and incidence along the trenches to $\phi=90^\circ$.

To access the reflectivity properties of individual lattices, the image of the sample was strongly magnified (1:20) and brought to an intermediate focus on a pinhole with a 0.5mm radius aperture. The transmitted light was then refocused on the slits of a spectrometer, dispersed and then detected by a cooled Ge photodiode. A polarisation rotator and a linear polariser were placed before the spectrometer to enable detection in both TE_{out} as well as TM_{out} polarizations.

III. DETERMINATION OF PHOTONIC BAND STRUCTURE

The photonic band structure of the lattices was first determined from the positions of sharp coupling features in the reflectivity spectra as a function of both polar θ and azimuthal ϕ angles see Fig.1 (a). The measurements in this section were performed in the polarizing conserving geometry ($\text{TE}_{\text{in}}, \text{TE}_{\text{out}}$). The results were compared with theoretical spectra obtained by numerical solution of Maxwell's equations by scattering

matrix techniques [7] and with band structures calculated by standard plane wave techniques [4,12].

A. Polar Angle Dependence

Reflectivity spectra as a function of polar angle are presented in the left side of Fig.2(a) for incidence perpendicular to the air trenches ($\phi=0^\circ$). The polar angle is varied in the range $15^\circ \geq \theta \geq 60^\circ$ in 5° steps. Two sharp resonant features (5-10 meV linewidth), superimposed on a slowly oscillating background are observed, arising from coupling to TE modes of the photonic band structure. Both bands shift down in energy by approximately 150meV from 15 to 60° as a function of angle, as indicated by the dashed lines on the figure.

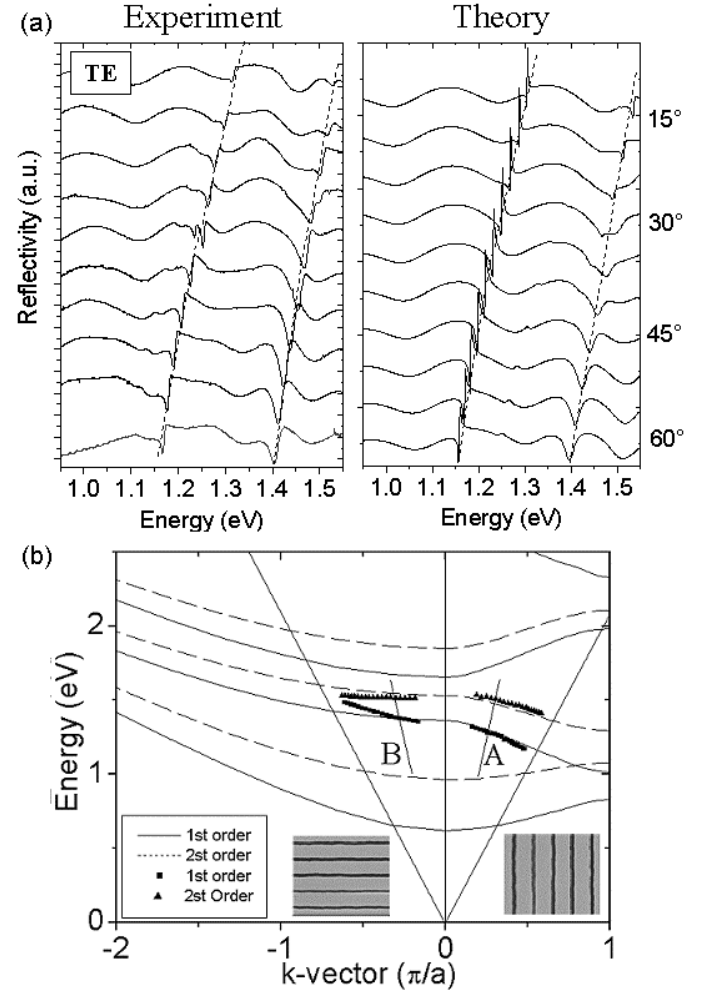


Fig 2. (a) Experimental and theoretical reflectivity as a function of polar angle θ for incidence perpendicular to the air trenches, $\phi = 0^\circ$. (b) Schematic of the band structure along two main symmetry directions: positive k -vectors represent the first photonic Brillouin zone for incidence perpendicular to the air trenches, negative k -vectors represent dispersions for incidence along the air trenches, $\phi = 90^\circ$. Dashed construction lines show the accessible light cone with external coupling techniques. The points labelled A and B correspond to the polar angle of 25° , and azimuthal angles 0 and 90° in Fig 3. Along the symmetry directions all modes are either pure TE or TM. Therefore no polarisation conversion occurs.

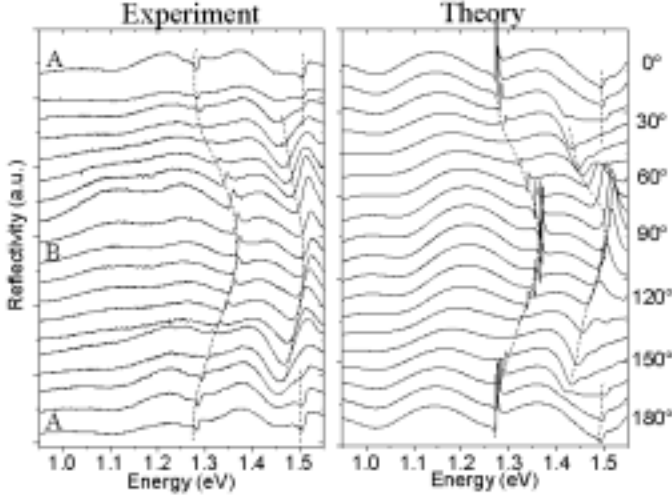


Fig 3. Experimental and theoretical reflectivity as a function of azimuthal angle in the range $0^\circ \leq \phi \leq 180^\circ$ in 10° steps for a fixed polar angle $\theta = 25^\circ$. The lower energy mode is 1st order and the higher energy mode 2nd order.

Simulations of the reflectivity spectra were carried out with the values of the parameters a , f , d and d_{cl} given in Sec. II.A. Very good agreement with experiment is obtained, as seen by comparison of the left and right sides of Fig.2(a). Calculations of the electromagnetic energy density in the vertical direction further show that the lower and higher energy bands correspond to 1st and 2nd order modes (see the field profiles in Fig.1(d)), respectively. As mentioned in the introduction, the features observed in surface reflectivity arise from coupling to leaky modes, due to scattering into the cladding and air. However, the 1st order mode only leaks very weakly, due to its better vertical confinement, thus leading to the observed sharper features in reflectivity. In order to obtain confinement of the higher order mode in the calculations, a reduced average refractive index 2.6 for the high Al concentration cladding layer was employed, to account for the expected presence of low index Al_xO_y around the air trenches [1,2].

The band structures shown in Fig.2 (b), both parallel and perpendicular to the trenches, were calculated using standard plane wave techniques, employing a simplified model of two perfectly reflecting mirrors with effective separation d^* , which is varied to account for vertical confinement to obtain the best fit to the data [4-6]. Values selected for the effective thickness were $d^* = 315\text{nm}$ for the 1st order and $d^* = 200\text{nm}$ for the 2nd order modes. The dispersions for incidence perpendicular to the trenches are determined by the photonic lattice potential. The dispersions parallel to the trenches can be understood physically as arising from a combination of the $k = 0$ quantized energies from the photonic lattice, together with an additional contribution from free propagation along the trenches, as represented by:

$$E = \left[E_m^2 + \left(\hbar c k_{\parallel} / 2\pi n_{eff} \right)^2 \right]^{1/2}, \text{ where } E_m \text{ is the energy of}$$

the mode at $k=0$ and n_{eff} is an effective refractive index. Use of this simple perturbation treatment gives a good fit (not shown

here) to the data for incidence parallel to the trenches.

Coupling to the resonance features occurs at the phase matching condition with conservation of in-plane wavevector given by $k = \omega/c \sin \theta$. Using this correspondence between k and θ , the angular dispersions of Fig.2(a) can then be plotted directly on the band structures of Fig.2(b) (the dots), with good agreement again being obtained between experiment and theory.

B. Azimuthal Angle Dependence

The dependence of the reflectivity spectra on azimuthal angle is shown in the left hand part of Fig.3 for ϕ from 0 to 180° in 10° steps for a fixed polar angle $\theta = 25^\circ$; corresponding theoretical spectra are shown on the right hand side. The sharp coupling features exhibit a shift by $\sim 100\text{meV}$ to higher energy as ϕ increases from 0° to 90° followed by a symmetrical shift to lower energy for further increase of ϕ up to 180° , behavior expected from the symmetry properties of the lattice (see Fig 2(b) insets). The variation from $\phi = 0^\circ$ to $\phi = 90^\circ$, at a fixed θ of 25° , corresponds to azimuthal rotation between points A and B on the polar-angle-variation band structure diagram of Fig 2(b). It is interesting to note that for arbitrary direction of incidence (ϕ), the modes excited in the waveguide have propagation direction different from that of the incident wave, an example of the very strong refractive properties of photonic crystals [14]. The direction of propagation is determined by the phase-matching condition in vector form [14] $\mathbf{k}_w = \mathbf{k}_i + \mathbf{G}$, where \mathbf{k}_w is the wavevector in the guide, with magnitude $(2\pi/\lambda)n_{eff}$, \mathbf{k}_i is the in-plane incident wavevector of magnitude $k_i = (\omega/c)\sin\theta$, and \mathbf{G} is the reciprocal lattice vector of the grating of magnitude $2\pi/a$. The direction of \mathbf{k}_w coincides with \mathbf{k}_i only in the case of incidence perpendicular to the trenches at $\phi=0, 180^\circ$.

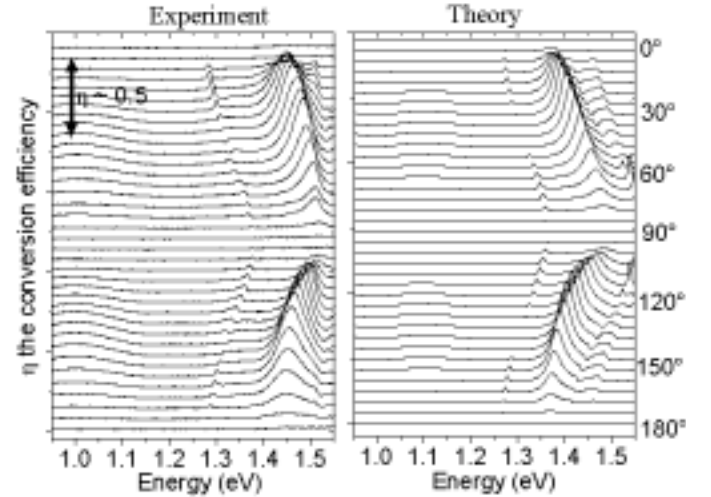


Fig 4. Experimental and theoretical azimuthal dependence of the polarization conversion ($\eta(E)=\text{TM}_{out}/\text{TE}_{in}$) spectra for a polar angle of $\theta = 25^\circ$. The azimuthal angle is varied from $0^\circ \leq \phi \leq 180^\circ$ in 5° steps. There is no polarization conversion along crystal symmetry directions at $\phi = 0^\circ, 90^\circ$ and 180° .

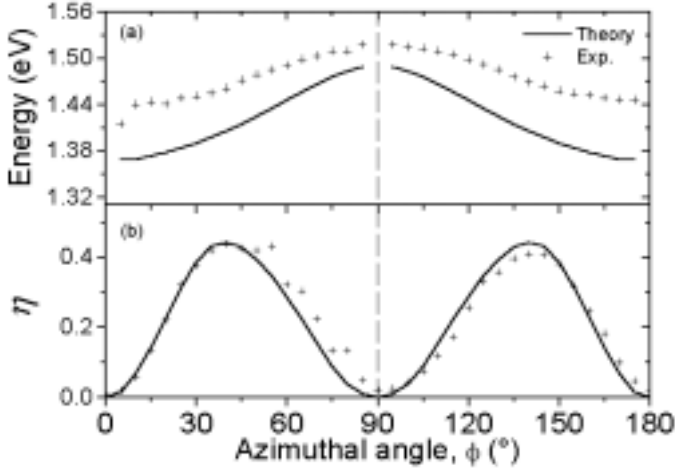


Fig 5. (a) Experimental and theoretical dependence of (a) the energy and (b) the amplitude of the main peak in the polarization conversion efficiency η (from Fig.4) as a function of azimuthal angle.

The calculated spectra in Fig.3 reproduce all the important features of the experiment, including the energy shift of the resonances with ϕ , the energy difference between the 1st and 2nd order features and even the spectral shape of the resonances. The good agreement with the calculations, together with that in Fig 2(a), clearly indicates that the theoretical model describes very well the band structures and coupling properties of the photonic crystal waveguides under investigation.

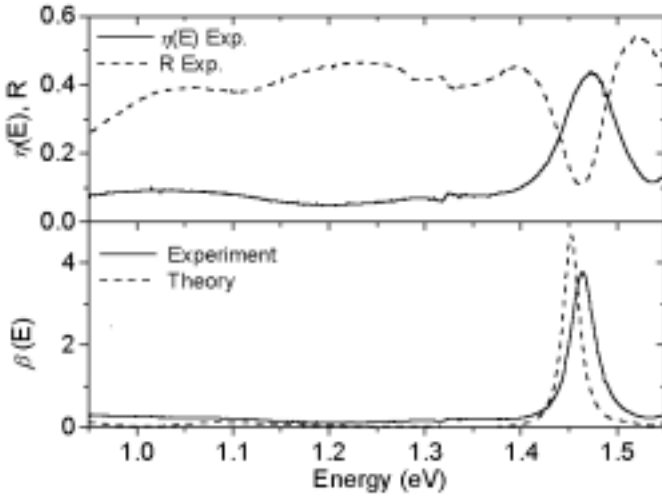


Fig 6. Experimental spectra for normalized reflectivity $R=TE_{out}/TE_{in}$, polarization conversion efficiency $\eta(E)=TM_{out}/TE_{in}$ and polarization degree $\beta(E)=TM_{out}/TE_{out}$ at $\phi=45^\circ$ and $\theta=25^\circ$. The results of scattering matrix calculations for $\beta(E)$ are shown for direct comparison.

IV. POLARIZATION CONVERSION EFFECTS

Experimental Results, Modelling and Discussion

Reflectivity spectra for TM_{out} detection (for TE_{in} incident polarization) are shown in the left part of Fig.4 for azimuthal angles ϕ from 0° to 180° , for the polar angle θ of 25° as in Fig.3. Once again theoretical spectra are shown for

comparison in the right half of the figure. The TM_{out} signal was normalized to the incident intensity (TE_{in}) by replacing the sample with a mirror and measuring TE_{out} ($=TE_{in}$ for the mirror). The normalized data in Fig.4 thus represent the polarization conversion efficiency ($\eta(E)$) as a result of reflection by the photonic lattice, with $\eta(E)$ given by the ratio TM_{out}/TE_{in} .

The important points of Fig.4 are as follows:

i) The energies and angular dependence of the peaks in Fig.4 are the same as for the resonances in Fig.3, thus showing that the polarization conversion arises from coupling to the photonic band structure modes. The angular variation of the energy of the main feature of Fig.4 is shown in Fig.5(a).

ii) There is no polarization conversion for incidence along the main lattice symmetry directions ($\eta=0$ for $\phi=0^\circ$, 90° and 180°), as seen in Fig.5(b).

iii) The conversion efficiency $\eta(E)$ is maximum at $\phi=45^\circ$ from the main symmetry directions. Along these directions it reaches the high level of $\eta(E)\sim 40\%$ at the resonant energies, as seen from Fig.5(b).

iv) Most importantly, at these resonant energies, and at $\phi=45^\circ$, the outgoing light is very strongly polarized, with the degree of polarization of the reflected light ($\beta(E)=TM_{out}/TE_{out}$) reaching very high levels up to 4 (i.e. 80% polarized). This is illustrated in the spectra of Fig.6 where TE reflectivity, $R=TE_{out}/TE_{in}$, $\eta(E)$ and $\beta(E)$ are presented. Inspection of Fig 6 shows that the very large values of β , the polarization of the reflected light arises partly because of the efficient conversion (high η), but also because the spectral feature in TE_{out} reflectivity exhibits a very strong resonant minimum (as opposed to the TM_{out} maximum).

All the results of Fig.4-6 were again modelled using scattering matrix calculations [7], with the theory results presented on the figures for direct comparison with experiment. As for the polar and azimuthal dependences for TE_{in}/TE_{out} , the calculations are found to describe very well the symmetry properties, spectral dependence and magnitudes of the polarization conversion effects.

The observed effects arise from the phenomenon of polarization mixing of TE/TM bands occurring for directions of incidence away from the symmetry directions of the 1D lattice. This effect, which results in TE_{in} incident light being reflected in TM_{out} polarization, is strongly enhanced at resonance frequencies where strong coupling to the photonic lattice occurs.

As mentioned briefly in the introduction, TE and TM states are pure, unmixed eigenstates in infinite 2D lattices. Along main symmetry directions, the introduction of symmetrical vertical waveguide confinement (as in an air bridge structure) leads to TE/TM mixing between bands of differing vertical parity (i.e. between 1st and 2nd order modes), as we discuss in ref [11]. In asymmetric structures with air above and dielectric cladding below, the modes no longer have definite parity and TE/TM mixing can occur between e.g. two 1st order modes. This is the origin of the weak anti-crossings between TE and TM bands we have reported along main symmetry directions for 2D lattices, and the observability of TE bands in TM polarization and vice versa [4]. However, by going away from the main

symmetry directions ($\phi \neq 0^\circ$ or 90°), much stronger polarization mixing and conversion becomes allowed, as we report here for the 1D lattices.

We have carried out simulations of the degree of polarization of the reflected light (β) as a function of etch depth. For shallow 1D gratings, as employed in e.g. grating couplers or fibre Bragg gratings, we find β of only 0.01 at 10nm etch depth, and 0.08 at 50nm, showing clearly that in order to achieve strong polarization conversion, deep etched photonic lattices, with strong modulation of refractive index must be employed.

V. CONCLUSIONS

Surface coupling techniques have been applied to study propagation and scattering phenomena in deep etched photonic crystal waveguides. Strong TE/TM polarization conversion of the reflected beams, arising from the periodic patterning and the vertical waveguide confinement of the photonic lattices has been reported. Polarization of the outgoing light of up to 80%, of opposite polarization to that of the incident light, has been found in non-optimized structures. These effects have a resonant character with finesse up to 10^2 - 10^3 and angular selectivity of $\sim 1^\circ$, both desirable properties for integrated optoelectronics applications. Furthermore, the experimental and theoretical techniques developed in this work are direct means to obtain in-depth information on photonic band structures, fabrication non-uniformities, and scattering and waveguiding properties of photonic crystal structures.

REFERENCES

- [1] T. F. Krauss, R. M. De La Rue and S. Brand, "Two-dimensional photonic-bandgap structures operating at near-infrared wavelengths", *Nature* (London), Vol. 383, pp.699-702 (1996)
- [2] V. N. Astratov, R M Stevenson, M S Skolnick, D M Whittaker, S. Brand, I Culshaw, T. F. Krauss, R. M. De La Rue, O. Z. Karimov, "Experimental technique to determine the band structure of two-dimensional photonic lattices", *Inst. Elec. Eng. Proc. Optoelectron.*, Vol 145 pp398-402 (1998).
- [3] T. Fujita, Y. Sato, T. Kuitani and T. Ishihara, "Tunable polariton absorption of distributed feedback microcavities at room temperature", *Phys Rev B* Vol. 57, pp.12428-12434 (1998).
- [4] V. N. Astratov, D M Whittaker, I S Culshaw, R M Stevenson, M S Skolnick, T F Krauss and R M De La Rue, "Photonic Band Structure Effects in the Reflectivity of Periodically Patterned Waveguides", *Phys. Rev. B*, Vol.60, No.24, pp.R16255-16258 (1999).
- [5] V. N. Astratov, I S Culshaw, R M Stevenson, D M Whittaker, M S Skolnick, T F Krauss and R M De La Rue, "Resonant coupling of near-infrared radiation to photonic band structure waveguides", *J. Lightwave Technol.* Vol. 17, No.11, pp.2050-2057, 1999.
- [6] V. N. Astratov, R M Stevenson, I S Culshaw, D M Whittaker, M S Skolnick, T F Krauss and R M De La Rue, "Heavy Photon Dispersions in Photonic Crystal Waveguides" *Appl. Phys. Lett.*, v.77, No.2, pp.178-180 (2000).
- [7] D. M. Whittaker and I. S. Culshaw, "Scattering-matrix treatment of patterned multiplayer photonic structures", *Phys. Rev. B*, Vol. 60, No.4, pp.2610-2618, 1999.
- [8] V. Pacradouni, W. J. Mandeville, A. R. Cowan, P. Paddon, J. F. Young and S. R. Johnson, "Photonic band structure of dielectric membranes periodically textured in two dimensions" *Phys. Rev. B*, Vol. 62, No 3, pp 4204-4207 (2000).

- [9] S. G. Johnson, S Fan, P R Villeneuve, J D Joannopoulos and L A Kolodziejski, "Guided modes in photonic crystal slabs", *Phys. Rev. B*, Vol.60, No.8, pp.5751-5758 (1999).
- [10] P. Paddon and J. F. Young, "Two-dimensional vector-coupled-mode theory for textured planar waveguides", *Phys. Rev. B*, Vol.61, No.3, pp.2090-2101 (2000).
- [11] D. M. Whittaker, I S Culshaw, V N Astratov and M S Skolnick., "Photonic bandstructure of patterned wave-guides with dielectric and metallic cladding", *Phys. Rev. B*, Vol 65, No. 7, pp073102 (2001).
- [12] J. D. Joannopoulos, R. D. Meade, and J. N. Winn, *Photonic Crystals* (Princeton University Press, Princeton, New Jersey, 1995)
- [13] M. C. Netti, A Harris, J J Baumberg, D M Whittaker, M B D Charlton, M E Zoorob and G J Parker, "Optical birefringence in photonic crystal waveguides" *Phys. Rev. Lett.* Vol. 86, No.8, pp.1526-1529 (2001).
- [14] Y. Zhao, I. Avrutsky, and B. Li, "Optical coupling between monocrystalline colloidal crystals and a planar waveguide", *Appl. Phys. Lett.*, Vol.75, No.23, pp.3596-3598 (1999).